

A COMPARISON OF FOUR METHODS FOR ACCURATE ULTRASONIC RANGE ESTIMATION

Billur Barshan and Birsal Ayrulu

Department of Electrical Engineering
Bilkent University 06533 Bilkent, Ankara, Turkey

ABSTRACT

Four methods of range estimation for airborne ultrasonic systems—namely simple thresholding, curve-fitting, sliding-window, and correlation detection—are compared on the basis of bias, standard deviation, total error, robustness to noise, and the difficulty of implementation. Whereas correlation detection is theoretically optimal, the other three methods can offer acceptable performance at much lower cost. Two variations of curve fitting and four variations of sliding-window have been considered. Performances of all methods are investigated as a function of target range, azimuth, and signal-to-noise ratio (SNR). Curve fitting, sliding-window, and thresholding follow correlation detection in the order of decreasing complexity. Apart from correlation detection, minimum bias and total error is most consistently obtained with the curve-fitting method. On the other hand, the sliding-window method is always better than the thresholding and curve-fitting methods in terms of minimizing the standard deviation of the estimate. The experimental results follow the simulations closely. Overall, the three simple and fast estimation methods provide a variety of attractive compromises between estimation accuracy and system complexity.

1. INTRODUCTION

Successful operation of most ultrasonic ranging systems relies on accurate *time-of-flight* (TOF) estimation. A pulse is transmitted and an echo is produced when the transmitted pulse encounters an object. The TOF t_o is the time elapsed between the transmission of a pulse and its reception, from which the target range can be calculated as $r = \frac{ct_o}{2}$, given the speed of sound in air c . Correct target localization using ultrasonics depends on how accurately TOF can be estimated, and how well c is known. In this paper, we consider three fast and simple suboptimal methods of TOF estimation which are compared to the optimal *correlation detection* on the basis of bias, standard deviation, total error, robustness to noise, and computational complexity.

2. TIME-OF-FLIGHT ESTIMATION

In widely-used *simple thresholding* systems, a range value r is produced when the echo amplitude first exceeds a preset threshold level τ (Fig.1).

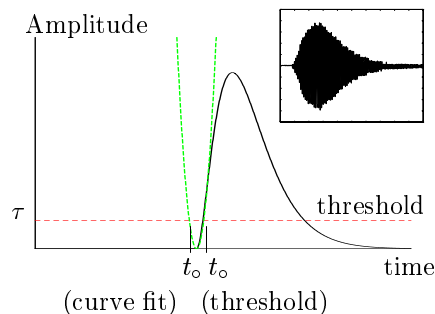


Figure 1: Echo envelope and TOF estimation by thresholding and curve fitting. *Inset*: Typical echo.

The main problem with this method is that the TOF estimate obtained is, on the average, larger than the true TOF, which corresponds to the starting point (onset) of the echo signal. This is a consequence of the relatively long rise-time of the echoes produced by currently available low-bandwidth ultrasonic transducers for operation in air. Hence, the range information obtained by simple thresholding is biased, making the target appear slightly farther than it actually is. The resulting bias error, which is in the range of several millimeters to centimeters, could easily be avoided if it were constant. However, this is not the case: The bias is difficult to model analytically since it is a function of τ , SNR, target location, size, and type, as well as other factors [1] causing amplitude fluctuations.

Another TOF estimation method is *curve fitting*, in which the Levenberg-Marquardt nonlinear least-squares method [4] is employed to fit a parabolic curve of the form $a_o(t - t_o)^2$ to the onset of the echo to produce an unbiased estimate. It has been verified in [2, 3] that the parabola is a good approximation for the onset of the signal. The vertex of the parabola is taken as the TOF estimate (Fig.1), which usually falls to the left of the thresholding estimate, reducing the bias considerably.

The authors of [3] have employed a simpler but less robust version of curve-fitting that does not require the nonlinear iterative fitting procedure: Two different threshold levels τ_1 and τ_2 ($\tau_2 > \tau_1$) are set, and the vertex of the parabola passing through the two signal samples at which τ_1 and τ_2 are exceeded is found as:

$$t_o = \frac{\sqrt{\tau_2/\tau_1} t_1 - t_2}{\sqrt{\tau_2/\tau_1} - 1}. \quad (1)$$

Here, t_1 and t_2 are the time samples at which τ_1 and τ_2 are exceeded. A threshold ratio τ_2/τ_1 of about 2 represents a suitable choice [3]. In the following, to distinguish the two approaches, we will refer to the original iterative least-squares curve-fitting method as CUF(A) and the 2-point analytical curve-fitting method as CUF(B).

The third method considered is the *sliding window*, whose use for ultrasonic signals was first suggested in [5]. The method originates from the *m*-out-of-*N* detection for radar signals [6]. A window of width *N* is slid through the echo signal one sample at a time, and the number of samples exceeding τ is counted at each window position. If this number exceeds a second threshold *m*, then a TOF estimate is produced. The advantage of the method is its robustness to noise spikes of duration less than *m* since detection is based on at least *m* samples exceeding τ , instead of a single one as in simple thresholding. We have considered four variations of choosing the TOF: SW(A): the very first sample of the window, SW(B): the first sample exceeding τ , SW(C): the sample at the center of the window, and SW(D): the $(N - m)$ th sample of the window.

The *optimum correlation detection* method produces an unbiased TOF estimate and maximizes the SNR which is taken as the ratio of the maximum amplitude of the echo signal to the amplitude noise standard deviation. A matched filter that contains a replica of the echo waveworm is employed to determine the most probable location of the echo in the received signal. The computer implementation of this procedure is time consuming because of the required correlation operation. Since the shape of the echo usually changes during propagation due to attenuation, and also varies with target type, size, location, and orientation, a large number of templates for the expected signal must be stored for the correlation operation. Another fundamental problem with this method is the inherent time delay involved since classical correlation detection requires that the *entire* echo be observed before an estimate is produced. Hence, when working in real time, this method is only suitable for distant objects when the echo duration is negligible compared to the travel time. For nearby targets, or in those applications where only the leading edge of the signal is available [7], the

estimate must be made at the beginning of the observed echo, using methods such as those described above. Nevertheless, this method serves as a useful basis for comparison of the other methods.

3. SIMULATION STUDIES

For a target at range *r* and azimuth θ in the far zone of the transducer, the received time signal can be approximated by the following signal model which is capable of representing observed signals for a wide variety of target types and locations [2]:

$$s_{r,\theta}(t) = k(r) e^{-\frac{\theta^2}{2\sigma_\theta^2}} (\Delta t)^2 e^{-a_1 \Delta t} \sin(2\pi f_o \Delta t) u(\Delta t) \quad (2)$$

Here, $\Delta t \triangleq t - t_o$, f_o is the resonance frequency of the ultrasonic transducers, $k(r)$ is a function of the target type and range [2], a_1 is a shape parameter of the signal, and $u(\Delta t)$ is the unit step function delayed by t_o . The angular beam profile is modeled as a Gaussian function with suitably chosen standard deviation σ_θ .

First, we consider the problem of finding suitable values for *N* and *m* in the sliding-window method. The intervals $5 \leq N \leq 50$ and $1 \leq m \leq N$ are searched for a wide range of *r* and θ values. We have observed that $N = 40$ and $m = 10$ are suitable choices for the range of parameters considered, and used these values throughout this study.

In the simulations, the values $f_o = 40$ kHz, $c = 343.5$ m/s, $\sigma_\theta = 27^\circ$, and $a_1 = 7050$ are used to model the echo signals obtained with Panasonic transducers. The value of τ is taken as 5 times the amplitude noise standard deviation in all the suboptimal methods. The value of *r* is varied from 0.25 m to 5.0 m with 0.25 m increments, and θ from 0° to 55° with 5° increments.

To estimate the bias and the standard deviation, 100 realizations are generated by adding zero-mean white Gaussian noise to the signal. A comparison among the various methods is made in Fig.2 and Table 1. We have considered the three options of processing the original signal modeled by Eq.(2) (O), the rectified signal (R), and its envelope (E). The total error \mathcal{E} is the root-mean-square value of the difference between the range estimate and the true range value. The bias *b* is the signed average of the same difference. These are related by $\mathcal{E}^2 = b^2 + \sigma^2$, where σ is the standard deviation.

Figs.2(a)-(f) show the dependence of bias, standard deviation, and total error on *r* and θ . The data for all combinations of *r*, θ are not presented due to space limitations; parts (a)-(c) are for $\theta = 0^\circ$ and parts (d)-(f) are for $r = 0.5$ m. The figures indicate that increasing *r* and $|\theta|$ degrades the estimation accuracy. Since the noise level is kept constant, this degradation is mostly caused by the decreasing SNR due to the decrease in

signal amplitude with increasing r and $|\theta|$ (Eq.(2)). For example, when the target at $r = 0.5$ m is moved from $\theta = 0^\circ$ to $\theta = 55^\circ$, SNR changes from 35 dB to 17 dB. Similarly, when the target is moved from $r = 0.25$ m to $r = 5$ m along the line of sight ($\theta = 0^\circ$), SNR changes from 41 dB to 15 dB. It can be observed that $|b|$ and \mathcal{E} of CUF(A) increases much more slowly with r and $|\theta|$, making it an attractive choice compared to the other methods which exhibit very large bias and total error for certain values of r and θ .

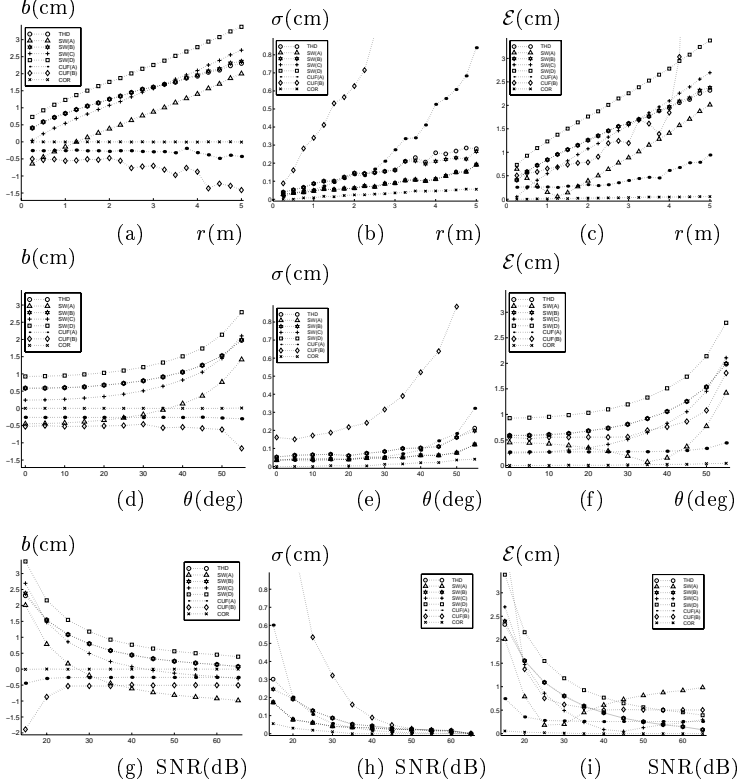


Figure 2: b , σ , and \mathcal{E} vs. r , θ , and SNR when the signal envelope is used. THD: thresholding, SW: sliding window, CUF(A): least-squares curve fitting, CUF(B): analytical curve fitting, COR: correlation.

Figs.2(g)-(i) illustrate the dependence of the performance directly on the SNR while the target is at $r = 0.5$ m and $\theta = 0^\circ$. SNRs between 15–65 dB have been realized by varying the amount of noise on the signal. Around 14 dB, the signal amplitude falls below τ , and a TOF estimate cannot be produced. In comparing the various methods, our purpose is to determine the method(s) which most consistently result in the best performance, over the range of r , θ , and SNR. This is because, even if we know the noise level, the signal level and thus the SNR will depend on r and θ , which are the very quantities one is trying to estimate.

We begin our comparison of the several methods by comparing the four variations of the sliding window

method among themselves. For all forms of the signal (i.e., O, R, or E), sliding-window (A),(C),(D) have equal σ as expected. This is because for a given N , the points taken as TOF in these variations (the very first, central, and the $(N - m)$ 'th samples of the window) remain fixed with respect to each other. Variation (B), on the other hand, exhibits a larger σ than (A), (C), and (D). For larger values of r or $|\theta|$, or smaller values of SNR, we observe that variation (A) gives the smallest bias, followed by variations (B), (C), and (D) in the given order. Among the sliding-window variations, (B), (C) and (D) would never be used since (A) can offer the same σ with smaller bias error than (C) and (D), and it can offer both smaller b and σ than (B). Thus, sliding window (A) emerges as the method of choice for larger r or $|\theta|$, or smaller SNR. This conclusion follows regardless of the relative importance attached to minimizing $|b|$ and σ . For smaller r or $|\theta|$, or larger SNR, the situation is more complicated and none of the variations is clearly superior to the others.

The bias errors of both sliding-window and thresholding methods increase with r and $|\theta|$. In contrast, the bias of CUF(A) is relatively constant over the r , θ and SNR values considered, and is generally smaller. It is followed by CUF(B), and the other methods.

On the other hand, the standard deviation of CUF(B) is the largest, followed by CUF(A) at SNRs below 20 dB, and by thresholding and SW(B) at SNRs above 20 dB. Apart from the correlation method, smallest standard deviations are obtained with SW(A),(C),(D). Therefore, in terms of standard deviation, curve-fitting methods are not as good as the sliding window method.

The total error \mathcal{E} turns out to be dominated by the bias and therefore has a shape which resembles the bias curve. In terms of bias and total error, CUF(A) shows the overall best performance. Although some of the variations of the sliding window result in smaller bias and total error over certain intervals, it would not be practical to exploit this since one does not know r and θ to begin with. Thus, we conclude that CUF(A) is the method which most consistently results in the lowest bias and total error over the range of parameters considered. In those instances where σ is more important than b and \mathcal{E} , the method of choice would be SW(A).

In order of increasing computational complexity, the methods can be sorted as thresholding, sliding-window, curve fitting, and correlation detection. For the processing of a single echo, the required CPU times on a SUN SPARC 20 workstation are 5.6 ms, 8.3 ms, and 11.1 ms for the first three methods respectively. The classical correlation detection method requires many orders of magnitude greater time if the correlation method is performed at every possible sample shift; in other

words if it is used as a detection method. In a practical implementation, the detection of the pulse can be performed by first thresholding and then applying the correlation only in the vicinity of the point where τ is exceeded, to get an accurate TOF estimate. Although such a hybrid thresholding/correlation method would be faster in a practical situation, it would still be difficult to implement, owing to the need to store many different templates which represent different points in the target position space.

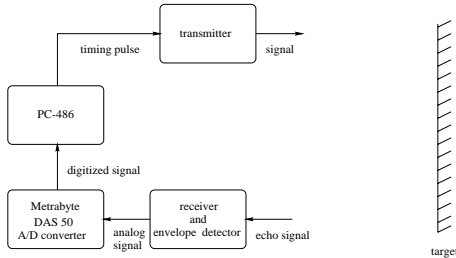


Figure 3: Block diagram of the data acquisition system.

4. EXPERIMENTAL RESULTS

Experiments are performed with Panasonic transducers, resonant at $f_o = 40$ kHz and exhibiting a relatively large half beamwidth of approximately 60° [8]. A planar target is positioned at $r = 0.5$ m and $\theta = 0^\circ$. The block diagram of the experimental setup is provided in Fig.3. Data acquisition is accomplished by using a 12-bit 1 MHz PC A/D card. 5,000 signal samples are collected, sampling at 500 kHz. Echo signals are post-processed on a SUN SPARC 20 workstation. Averages over 100 noisy signals are computed to produce the correlation templates for O, R, and E. Experimentally obtained b , σ , and \mathcal{E} values for all four methods, computed over 100 echo signals, are presented in Table 1.

method		simulation			experiment		
		b (cm)	σ (cm)	\mathcal{E} (cm)	b (cm)	σ (cm)	\mathcal{E} (cm)
THD	O	0.671	0.0822	0.676	0.585	0.0793	0.590
	R	0.666	0.0843	0.672	0.582	0.0790	0.587
	E	0.586	0.0524	0.588	0.576	0.0624	0.579
SW(A)	O	-0.228	0.0394	0.231	-0.229	0.0449	0.233
	R	-0.232	0.0415	0.235	-0.227	0.0449	0.231
	E	-0.448	0.0348	0.449	-0.423	0.0377	0.425
SW(B)	O	0.671	0.0822	0.676	0.585	0.0793	0.590
	R	0.666	0.0843	0.672	0.582	0.0790	0.587
	E	0.586	0.0524	0.588	0.519	0.0681	0.523
SW(C)	O	0.459	0.0394	0.461	0.460	0.0449	0.462
	R	0.455	0.0415	0.457	0.458	0.0449	0.460
	E	0.239	0.0348	0.241	0.225	0.0322	0.227
SW(D)	O	1.146	0.0394	1.147	1.147	0.0449	1.148
	R	1.142	0.0415	1.143	1.145	0.0449	1.146
	E	0.926	0.0348	0.927	0.912	0.0366	0.913
CUF(A)	O	0.436	0.242	0.499	0.428	0.227	0.484
	R	-0.269	0.0534	0.274	-0.216	0.0613	0.225
	E	-0.261	0.0345	0.263	-0.227	0.0361	0.230
CUF(B)	O	-0.578	0.301	0.652	-0.515	0.290	0.591
	R	-0.507	0.309	0.594	-0.472	0.283	0.550
	E	-0.530	0.161	0.554	-0.502	0.142	0.522
COR	O	0.000	< 0.0001	< 0.0001	-0.000344	0.0185	0.0185
	R	0.000	< 0.0001	< 0.0001	-0.00447	0.0298	0.0301
	E	0.000	< 0.0001	< 0.0001	-0.00523	0.0312	0.0316

Table 1: Simulation and experimental results for $r = 0.5$ m, $\theta = 0^\circ$, and SNR=35 dB.

5. CONCLUSION

Four range estimation methods are compared on the basis of bias, standard deviation, total error, robustness to noise, and difficulty of implementation. Correlation detection always gives the best results and forms a basis for comparison for the simpler and faster sub-optimal methods. However, it is also computationally the most complex, with certain disadvantages in a real-time implementation. Curve fitting, sliding-window, and thresholding follow correlation detection in the order of decreasing complexity and can offer acceptable performance at much lower cost. Performances of all methods have been investigated as a function of target range, azimuth, and SNR. Two variations of curve fitting and four variations of sliding-window have been considered. Apart from correlation detection, lowest bias and total error is most consistently obtained with least-squares curve-fitting applied to the signal envelope. However, when it is more important to minimize standard deviation than bias and total error, sliding window emerges as the method of choice. For all forms of the signal (i.e., O, R, E), sliding-window variations (A),(C),(D) have equal standard deviations which is also the smallest among all the methods. Depending on the relative importance of bias and standard deviation for a given application, the method of choice can be determined. Since bias is the dominant component of the total error, developing algorithms that are robust to bias errors are of interest. The experimental results are in very good agreement with the corresponding simulations. Overall, the three simple and fast estimation methods provide a variety of attractive compromises between estimation accuracy and system complexity.

6. REFERENCES

- [1] Cracknell A.P., *Ultrasonics*, Wykeham Publications Ltd., London, 1982.
- [2] Barshan B. and Kuc R., *IEEE T. Syst. Man. Cybern.*, 22(4):636–646, 1992.
- [3] McMullan W.G., Delanghe B.A., and Bird J.S., *IEEE T. Instrum. Meas.*, 45(4):823–827, 1996.
- [4] Press W.H., Flannery B.P., Teukolsky S.A., and Vetterling W.T., *Numerical Recipes in Pascal*, pp.574–579, Cambridge Univ. Press, U.K., 1989.
- [5] Barshan B. and Ayrulu B., *Electron. Lett.*, 34(16):1616–1617, 1998.
- [6] DiFranco J.V. and Rubin W.L., *Radar Detection*, Artech House, Dedham, MA, 1980.
- [7] Freitag L.E. and Tyack P.L., *J. Acoust. Soc. Am.*, 93:2197–2205, 1993.
- [8] Panasonic Corp. Ultrasonic ceramic microphones, Burlington, MA, 1989.